Journal of Computational Acoustics, Vol. 2, No. 3 (1994) 251–266

GLOBAL INVERSION BY GENETIC ALGORITHMS FOR BOTH SOURCE POSITION AND ENVIRONMENTAL PARAMETERS

PETER GERSTOFT
SACLANT Undersea Research Centre, 19138 La Spezia, Italy

The data set from the Workshop on Acoustic Models in Signal Processing (May 1993) is inverted in order to find both the environmental parameters and the source position. Genetic algorithms are used for the optimization. When using genetic algorithms the responses from many environmental parameter sets are computed in order to estimate the solution. All these samples of the parameter space are used to estimate the *a posteriori* probabilities of the model parameters. Thus the uniqueness and uncertainty of the model parameters are assessed.

1. Introduction

This paper is concerned with the solution of the test problems given at the Workshop on Acoustic Models in Signal Processing[1] by the use of a global inversion approach.[2]

Recently, there has been much concern over the degradation of matched field processing (MFP) due to environmental mismatch.[3–5] Therefore there has been an effort in the community to include some of the environmental uncertainty in the processing.[6–8] However, these methods all give special treatment to the source position by doing an exhaustive search over range and depth, and often they also include some *a priori* knowledge of the importance of the search parameters. Rather than *a priori* assuming anything about the importance of the parameters, we will initially treat all parameters identically and then let the algorithm adaptively adjust the search.

There has also been concern over constructing robust processors which will not cause degradation in performance due to environmental uncertainty. By doing a global search we are essentially using a very robust processor for the environment, even though we are using a very simple measure of the fit between the observed and predicted fields.

Finally, it is also recognized that when a solution has been obtained there should be some analysis of the accuracy and uncertainty of the solution. This could be done by calculating Cramer–Rao bounds,[9] convergence analysis,[6] or a probabilistic estimate of the solution.[7] When using global optimization methods the responses from many environmental parameter sets have to be computed in order to estimate the solution. Many samples of the models are used to estimate the *a posteriori* probabilities of the model parameters. Thus the uniqueness and uncertainty of the model parameters are assessed.

From the above discussion it is clear that a global optimization method does solve some of the problems in MFP. The global search method described by Gerstoft[2] is used. Contrary to classical source localization methods, no special attention is given to the source parameters. Thus the approach is very general and can be used for many other inversion problems. Genetic algorithms (see, e.g., Ref. 10) are used for the optimization and the results are displayed in terms of *a posteriori* probability distributions.

There is some concern over the CPU time which can be excessive when doing global optimization. Often MFP methods estimate the source location by doing exhaustive search in range and depth for several environments picked either by experience or randomly. For 40 environments and 50 range and depth points this gives $40 \cdot 50 \cdot 50 = 100{,}000$ parameter combinations or forward model runs. This is the same number as used for the global search in this paper, but estimates of the environment and an assessment of the accuracy of the solution are also obtained here. To limit the inversion time, a classical MFP may use just one environment, which in the example above corresponds to 2500 forward model runs. Global search methods are so flexible that they could also limit the computer time to 2500 forward models. Then a search would be performed over the source range and depth and, say, two of the most important environmental parameters. The state of the art of optimization is so advanced that usually it should not be necessary to do an exhaustive search.

2. Optimization using Genetic Algorithms

The nonlinear inverse problem is stated as an optimization problem: Find the model vector $\mathbf{m}$, or parameter set, that minimizes the quadratic deviation

$$\phi(\mathbf{m}) = 1 - \mathbf{p}^*(\mathbf{m})\mathbf{C}\mathbf{p}(\mathbf{m})/N_{\mathrm{rd}}\,, \tag{2.1}$$

where ϕ is the object function. The second term in this equation corresponds to the Bartlett processor. Normally, in genetic algorithms the object function is maximized, but here we minimize the object function defined by Eq. (2.1), to be in accordance with simulated annealing. Here $\mathbf{m}$ is the model vector consisting of the physical parameters, $\mathbf{p}$ is a vector containing the calculated pressure normalized to unit norm on the N_{rd} hydrophone depths, and $\mathbf{C}$ is the covariance matrix of the observed pressure on the array. The division by N_{rd} is due to the normalization of the observed covariance matrix in the present application. The calculated replicas are obtained by calling the forward modeling routine, here SNAP,[11] with the model vector $\mathbf{m}$ as input.

Global optimization methods accept that the object function is irregular and try to find the global minimum without doing an exhaustive search. An advantage of global optimization is that it only requires the value of the object function at arbitrary points in space and the problem can then be solved without any further knowledge of the object function. Thus, once the global inversion method has been tuned, any forward model can be used. Early solutions to the global problem were attempted using a simple Monte Carlo method, whereas modern methods use directional searches such as *genetic algorithms* (GA) or *simulated annealing* (SA).

Genetic algorithms are based on an analogy with biological evolution. While these have already provided promising results in the seismic community,[12–15] a first application to ocean acoustic problems was published only recently.[2] The basic principle of the GA is simple: From all possible model vectors, an initial population size of q members is selected. The fitness of each member is computed based on the fit between the observed data and the computed data. Then through a set of evolutionary steps the initial population evolves in order to become more fit. An evolutionary step consists of selecting a parental distribution from the population based on the individual's fitness. The parents are then combined in pairs and operators are applied to them to form a set of children. Traditionally the crossover rate and mutation rate operators have been used. Finally, the children replace part of the population to get a more fit population.

The environment is discretized into M parameters in a model vector $\mathbf{m}$. Each parameter m_j, $j = 1, \ldots, M$, can take 2^{n_j} discrete values according to an *a priori* probability distribution (Gaussian, rectangular, or based on *a priori* information). Here a rectangular distribution between a lower and an upper bound $[m_j^{\min}, m_j^{\max}]$ is used. We have (see Fig. 1)

$$m_j = m_j^{\min} + i_j \Delta m_j \,, \quad i_j = 0, \ldots, 2^{n_j} - 1 \,, \tag{2.2}$$

where

$$\Delta m_j = \frac{m_j^{\max} - m_j^{\min}}{2^{n_j} - 1} \,. \tag{2.3}$$

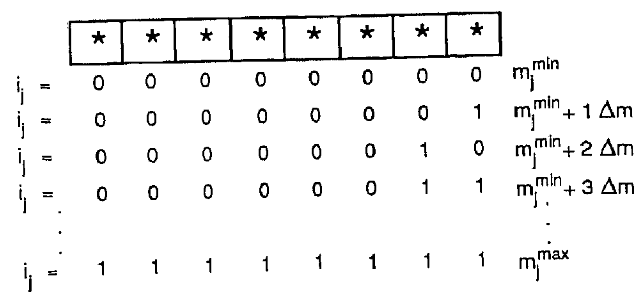

Fig. 1. Binary coding of model parameters.

A major difference between simulated annealing and GA is that GA is using q model vectors at the same time, where q is the population size, while simulated annealing only uses one. GA consists essentially of three operators: selection, crossover, and mutation.

Selection: In order to establish a new population, also with q members, fq parents must be selected, $0 < f < 1$. The choice is made with a probability proportional to the fitness of its members. The simplest probability is given by

$$p_k = \frac{1 - \phi(\mathbf{m}_k)}{\sum_{l=1}^{q} [1 - \phi(\mathbf{m}_l)]} \,, \quad k = 1, \ldots, q \,. \tag{2.4}$$

The introduction of a temperature, as in simulated annealing, gives us the opportunity to stretch the probability and to improve the performance of the algorithm.[14] Indeed, at the first stage of the procedure, by stretching the fitness we avoid to choose as parents only the members with the better fit, which would otherwise tend to dominate the population.

Later in the optimization, this stretching leads to a better discrimination between models with very close fitness. In order to take into account this new parameter, the probability is rewritten as

$$p_k = \frac{\exp[-\phi(\mathbf{m}^k)/T]}{\sum_{l=1}^{q} \exp[-\phi(\mathbf{m}^l)/T]}, \quad k = 1, \ldots, q. \tag{2.5}$$

But, as with simulated annealing, the choice of the temperature T is difficult. It must neither be too high nor too low. A good compromise is a temperature of the same magnitude as the object function; here $T = \min[\phi(\mathbf{m}^k)]$. During the optimization, the fitness and the temperature decrease.

Crossover: For each set of parents, each consisting of a model vector, two children are constructed, and for each parameter in the model vector each child may either be a direct copy of one parent, with probability $1 - p_x$, or it can be a bit crossover of the two parents with crossover probability p_x (see Fig. 2). The crossover point is chosen randomly in the interval $[1, N-1]$, where N is the number of bits used in the coding. Different techniques are available to perform this crossover of the population, e.g., single point crossover where the entire chromosome is used once and multiple point crossover where the chromosome is divided into genes related to each parameter on which the crossover is applied. Multiple point crossover is used here.

Mutation: This is a random change of one bit in the model vector, with probability p_m, in order to better explore the search space (see Fig. 3).

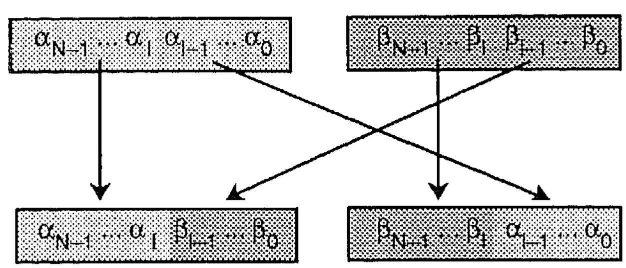

Fig. 2. Crossover is a binary exchange of l bits between the binary codes for two model parameters. l is chosen randomly.

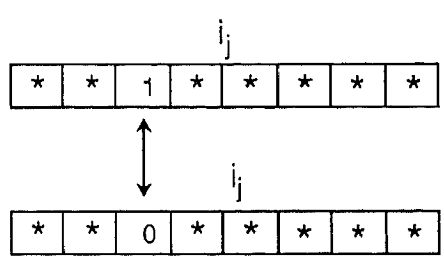

Fig. 3. Mutation is a random change of one bit.

It is possible that a run of a GA will approach a local minimum. In order to increase the probability of finding the global minimum, several independent populations M_{par} are started. This is also advantageous for collecting statistical information to estimate the probabilities as shown in the examples in the next section.

In the present implementation there are relatively few GA parameters which in principle have to be tuned for each application, and the precise value of each of these does not seem to be very important. We usually only vary M_{par} in order to adjust the execution time to the available CPU time. Based on our limited experience, the following values are recommended:

- The population size q should be large enough such that the model vectors can represent several minima, but also small enough such that several iterations can be performed; $q = 64$ seems to be a good compromise.
- The reproduction size f should be large enough such that the fittest individuals stay in the population during the iterations; f should be less than 0.9; here $f = 0.5$.
- The crossover rate depends on how independent the parameters in the model vector are. A crossover rate p_{x} close to 1.0 seems to be a good choice for independent parameters; for dependent parameters a lower value of p_{x} is recommended; here $p_{\mathrm{x}} = 0.8$.
- It has been found that a high mutation rate gives the best result; here $p_{\mathrm{m}} = 0.05$.
- The number of forward computations for each population should be relatively low (i.e. 1000–5000).
- The number of parallel runs M_{par} depends on the application. To obtain a reasonable estimate of the inversion parameters, $M_{\mathrm{par}} = 1$ is sufficient. For computing the probability distribution it must be larger, e.g., $M_{\mathrm{par}} = 50$.

3. *A posteriori* statistics

During the optimization, all the obtained samples of the search space are stored and used to estimate the *a posteriori* probabilities. For a system of M parameters the result is an M-dimensional space. This is difficult to display and we will only show the marginal probability distributions. The samples are ordered according to their energy and the probability distribution is scaled using the Boltzmann distribution as for the optimization.

The difficulty is to choose the value of the temperature: taking it equal to the fittest sample favors the fittest part of the samples, whereas taking it equal to the least fit penalizes the best fit. A good choice, shown by experience, is to use a temperature equal to the average of the best 50 samples. The probability for the kth model vector is then given by

$$\sigma(\mathbf{m}^k) = \frac{\exp[-\phi(\mathbf{m}^k)/T]}{\sum_{l=1}^{N_{\mathrm{obs}}} \exp[-\phi(\mathbf{m}^l)/T]} . \tag{3.6}$$

For the ith parameter in the model vector the marginal probability distribution for obtaining the particular value κ can be found by summing Eq. (3.6):

$$\sigma_i(m_i = \kappa) = \frac{\sum_{k=1}^{N_{\mathrm{obs}}} \exp[-\phi(\mathbf{m}^k)/T]\delta(m_i^k = \kappa)}{\sum_{k=1}^{N_{\mathrm{obs}}} \exp[-\phi(\mathbf{m}^k)/T]} , \tag{3.7}$$

where N_{obs} is the number of observed model vectors and T is the temperature.

The disadvantage of using the marginal *a posteriori* probability distribution is that they do not reflect the correlation between the parameters. By this method the model vectors with the best fit might not be retrieved, as the peaks in the probability distribution might not reflect a possible parameter combination. However, useful statistics can be retrieved.

4. Solution of the Test Cases

We solved the sound speed mismatch case (SSPMIS), the general mismatch case (GENLMIS) (see Fig. 4), and the sloping bottom case (SLOPE), not shown. For the sound speed mismatch only the sound speed in the water is varying, the other environmental parameters in Fig. 4 are fixed. The sloping bottom case is as in GENLMIS but the water depths at 0 and 10 km are unknown; we will only invert for the 'average' depth as seen by the field, thus it has the same number of parameters as the general mismatch case. The source frequency is 250 Hz. The source was known to be in the interval from 5–10 km in range and 0–100 m in depth. The two source parameters and the environmental parameters could take 51 discrete values for each parameter. For the four parameters in the SSPMIS case this gives a search space of $51^4 = 7 \cdot 10^6$ and for the nine parameters in the GENLMIS and SLOPE cases the search space is $51^9 = 2 \cdot 10^{15}$. Contrary to an inversion for environmental parameters where the source position is relatively well known, the uncertainties in the source depth and range were so large here that they became the most important parameters in the hierarchy of the parameters, and it was thus more challenging to find the environmental parameters.

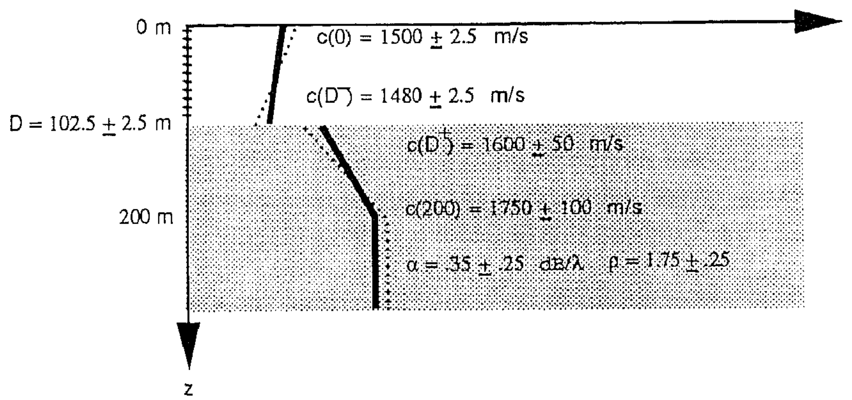

Fig. 4. The environment for the general mismatch case. The source frequency is 250 Hz and the source is located between 0–100 m in depth and 5–10 km in range. The vertical receiving array was spanning the water column with 20 receivers from 5 to 100 m.

Since the major part ($\approx$ 99%) of the CPU time is spent in forward modeling, it is important that the forward solution is computed efficiently. We have used a modified version of the SNAP code.[11] On a DEC-3000 Alpha workstation one forward solution (one set of source and environmental parameters) could be obtained in 0.15 s. This enables us to sample 50,000 models in 2 h (SSPMIS) and 125,000 models in 5 h (GENLMIS and SLOPE). These numbers are very small compared to the size of the search space but large enough such that we are sure of not getting trapped in a local minimum and that a good estimate of the probability distributions can be obtained.

The inversion of the data is done in two steps. First the optimization part is carried out to find the best parameter sets and their corresponding value of the object function for all the M_{par} parallel runs, and afterwards a postprocessor is run to estimate the *a posteriori* probabilities from the samples obtained during the optimization. For SSPMIS the optimization was done in $M_{\text{par}} = 40$ parallel runs each sampling 1250 models. For the GENLMIS and SLOPE we ran $M_{\text{par}} = 50$ parallel runs each sampling 2500 models. The population size was $q = 64$ and the reproduction rate was $f = 0.5$. The *a posteriori* probabilities were estimated from the best models at the final M_{par} populations, in total $M_{\text{par}}\, qf = 1280$ (SSPMIS) or 1600 (GENLMIS and SLOPE). The probability distribution is estimated by weighing the fitness according to a Boltzmann distribution, where the temperature is equal to the average fitness for the 50 best models.[2]

For the sound speed mismatch case all the true values of the source position and environmental parameters were found exactly.[1] From a global inversion point of view the search space here is rather small and this case (results not presented) is therefore not so interesting as the following test cases.

4.1. *General mismatch*

The environment could be discretized either by the parameters as given in Fig. 4, where the water sound speed is specified by its upper and lower speeds, or we could represent the water sound speed by a constant offset and a slope. The difference between the two discretizations is that the first is based on points whereas the last is based on a set of shape functions. These could be thought of as the first two functions in an expansion in terms of empirical orthogonal functions (EOF). Naturally, real EOFs are directly computed from observed sound speed profiles or based on archival data.[16] Using results from the first discretization it is seen that the discretization using shape functions is advantageous.

The value of the object function versus the upper and lower water speeds for the other parameters kept at their best values is displayed in Fig. 5(a). We see that the maximum is not confined to a single value of one of the speeds, but the best fit is obtained for a constant offset between the two values, i.e. the slope of the profile is important. Instead we could plot the 2D marginal *a posteriori* probability distribution between the lower and upper water speeds (Fig. 5(b)). The 2D marginal probability distribution is the projection of the M-dimensional probability distribution onto a plane, and the other parameters have thus not been fixed. The constant slope in Fig. 5(b) also indicates that these parameters are correlated.

Figure 5 shows that there is a strong correlation between the upper and lower sound speeds. It is easier to invert a set of uncorrelated parameters since a better fit can then be obtained by changing only one parameter as opposed to changing several parameters simultaneously. The water sound speed profile is clearly best modeled by a constant shape

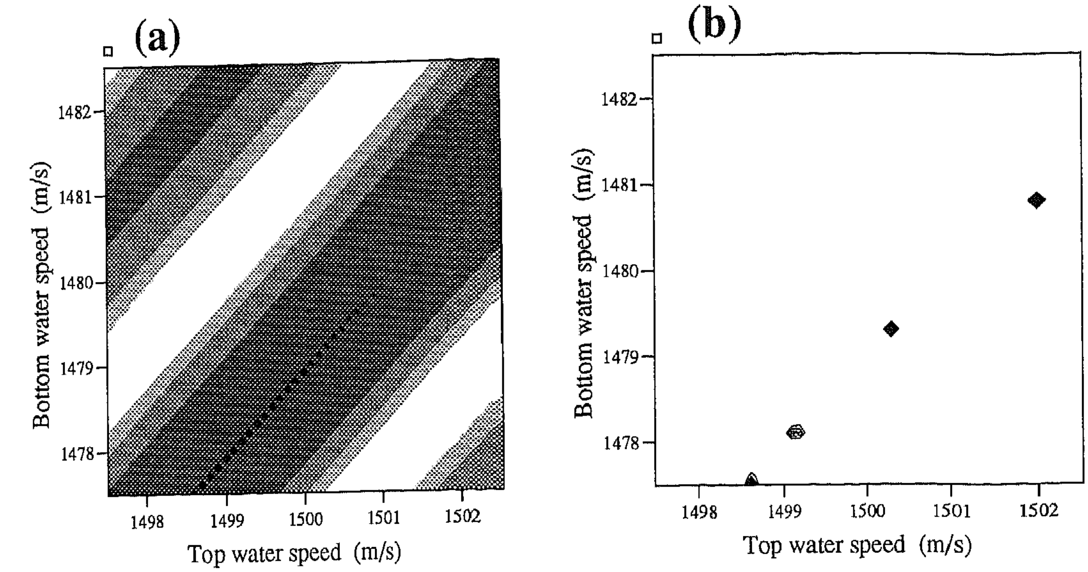

Fig. 5. (a) The value of the object function vs top and bottom water sound speeds (dark indicates a good fit). (b) 2D marginal probability distribution for top and bottom water sound speeds (dark indicates a high probability).

function plus a sloping shape function. The constant shape function is taken here as the speed at the top and the slope represents the decrease from this value at the bottom. The ranges of the two amplitudes are then 1497.5–1502.5 m/s and 15–25 m/s. This discretization is chosen in order to match the discretization initially specified.

For the 40 dB SNR we have carried out the inversion using both discretizations. The marginal *a posteriori* probability distributions for the two inversions are shown in Fig. 6. How well determined a parameter is can be seen from the height and the uniqueness of the marginal probability distribution. The curves are normalized so that the area under each curve is the same. The more well defined a distribution is the more likely it is to be close to the correct value for this parameter. The distribution is also an indication of the sensitivity of the parameter when the other parameters are varying. In both cases the source position is well determined. In Fig. 6(a) the water depth, the third most important parameter, is also well determined. The fourth most important parameter is the upper sediment speed which is determined at a value about 10 m/s from the correct value. Both the attenuation and the density have well defined, but flatter, distributions close to their true values. The lower sediment speed is not very well determined and the probability distribution spans the whole interval. For both the top and bottom water sound speeds there is considerable ambiguity in value and it is not clear which values are the optimal. As discussed above this reflects the fact that the absolute value of the sound speed is not important; only the decrease in sound speed is important.

The result of using shape functions for the water sound speed gives a high resolution of source range, source depth, water speed decrease, water depth, and upper sediment speed (Fig. 6(b)). Since the water sound speed profile has been better determined now, the parameters in the sediment can also be better resolved (see Fig. 6(a) compared to

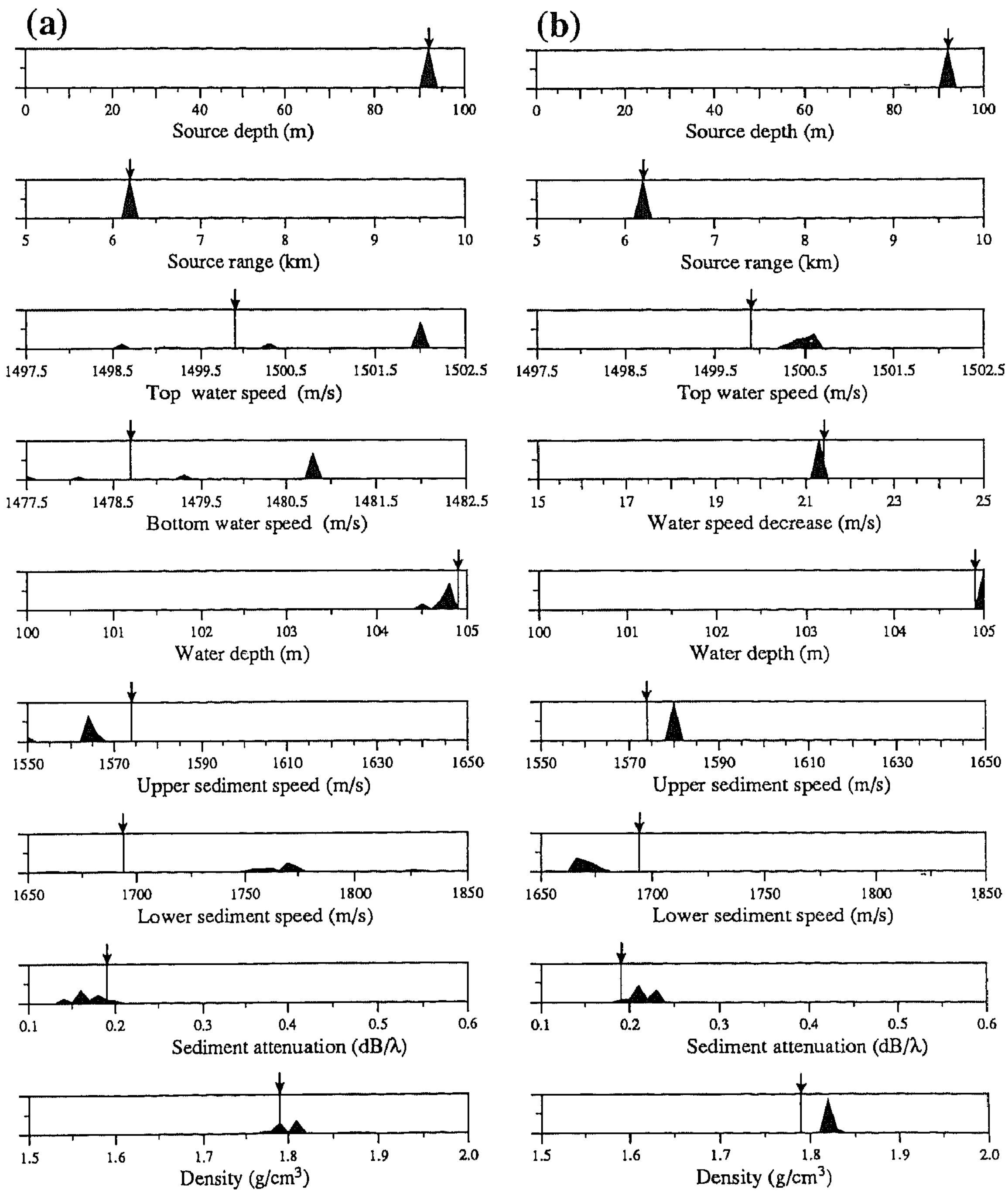

Fig. 6. Probability distribution for the general mismatch case based on the environment in Fig. 1 for the 40 dB SNR. (a) is based on the original discretization of the environment and (b) is based on shape functions. The arrows indicate the correct values.

Fig. 6(b)). For the given search interval for the parameters it can be seen from Fig. 6(b) that the constant value of the water sound speed (top water speed) is one of the least important parameters. This example shows that different results can be obtained depending on how the environment is discretized. The use of shape functions is clearly advantageous in this example for determination of environmental parameters.

It is clear from this example that reparametrization is important, but there are not yet general procedures to determine the reparametrization or to determine if a parameter is necessary for the inversion. As always physical insight is important; this can be further aided by the plotting of the marginal probability distributions (both 1D and 2D), the plotting of the object function versus two parameters, and the plotting of local error estimates[17] or the eigenvectors of the Fisher information matrix[18] (all work in progress).

If the background noise level is increased we expect a deterioration in our ability to determine the true parameters. For a SNR = 10 dB (Fig. 7(a)) we are still able to determine the correct source depth and range, though the range has a second peak in the probability function. The decrease of the sound speed in the water is well determined with two peaks close together. The less important parameters of the sediment as well as the absolute value of the water speed are not very well determined in this case. For a SNR = −5 dB (Fig. 7(b)) the source and the water sound speed decrease are well determined and the source range has a flat distribution close to the true value. The remainder of the parameters are undetermined.

To summarize, there are three possible estimates of the unknown parameter values:

(i) The parameter set with the best fit to the data during the optimization (best fit).
(ii) The maximum of each marginal *a posteriori* probability distribution (max ppd).
(iii) The mean of each marginal *a posteriori* probability distribution (mean ppd).

The last two methods have the disadvantage that they do not reflect a correlation between the parameters. When the inversion is 'easy' there is no difference between the three estimates, and this is an indication that a reliable solution has been obtained. This was the case for the 40 dB SNR case. The values of the three estimates for the −5 dB SNR case are shown in Table 1. The method using the best obtained fit has the source position correct and therefore a higher Bartlett power. Often this is the method that gives the best estimate and we will use it in the following.

For the three SNR's of the general mismatch case, the parameter values giving the best match to the data are shown in Table 2. For low SNR the sediment values are quite well determined, even though the probability distributions indicate that all values in the search interval are almost equally likely.

The source localization was done assuming a different environment for each SNR case. Alternatively, the environment found for the high SNR could be used again for the lower SNR's; the inversion is then reduced to finding the maximum of the ambiguity surface for the source position. Using this approach, the source position for the low SNR's was found exactly.

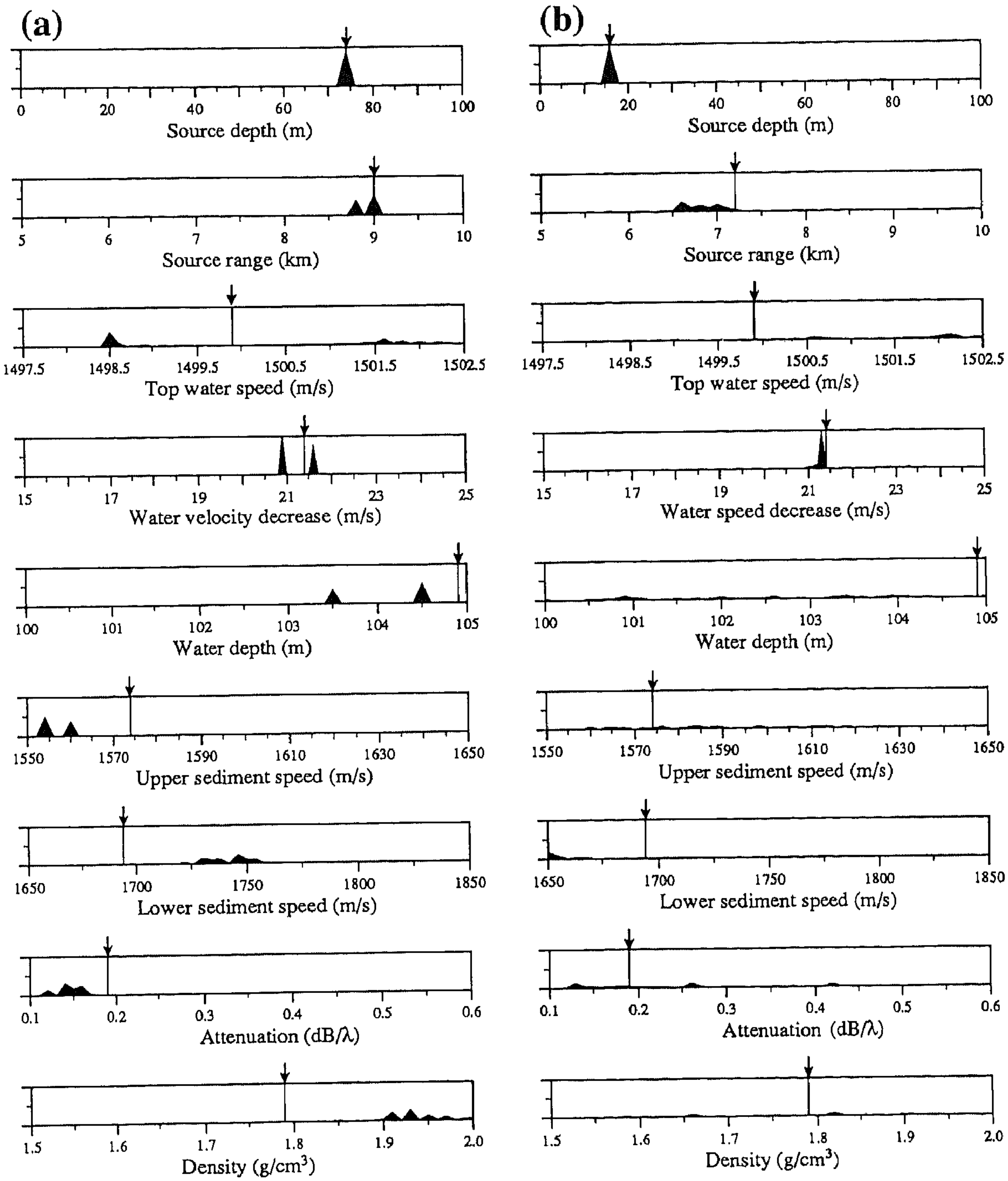

Fig. 7. Probability distribution for the general mismatch based on the discretization of the water speed by shape functions. (a) 10 dB SNR, (b) −5 dB SNR. The arrows indicate the correct values.

Table 1. Estimated parameters for the general mismatch SNR = −5 dB case using the three estimation methods (ppd: *a posteriori* probability distribution).

Parameter		Estimated values		
		Best fit	Max ppd	Mean ppd
Source depth	(m)	16	16	16
Source range	(km)	7.0	6.6	6.8
Top water speed	(m/s)	1502.2	1502.1	1501.2
Water speed decrease	(m/s)	22	21.3	21.7
Water depth	(m)	103.5	100.9	102.3
Upper sediment speed	(m/s)	1578	1576	1585
Lower sediment speed	(m/s)	1650	1650	1710
Attenuation	(dB/λ)	0.14	0.13	0.23
Density	(g/cm^3)	1.82	1.82	1.75
Bartlett power	(dB)	13.3	11.6	13.2

Table 2. The best fit parameters for the general mismatch case.

Parameter		Estimated values			True values		
		40 dB	10 dB	−5 dB	40 dB	10 dB	−5 dB
Source depth	(m)	92	74	16	92	74	16
Source range	(km)	6.2	9.0	7.0	6.2	9.0	7.2
Top water speed	(m/s)	1500.6	1498.5	1502.2		1499.9	
Water speed decrease	(m/s)	21.3	20.9	22.0		21.3	
Water depth	(m)	105.0	104.5	103.5		104.9	
Upper sediment speed	(m/s)	1580	1554	1578		1574	
Lower sediment speed	(m/s)	1666	1746	1650		1694	
Attenuation	(dB/λ)	0.21	0.14	0.14		0.19	
Density	(g/cm^3)	1.82	1.93	1.82		1.79	
Bartlett power	(dB)	13.0	13.0	13.3			

The best measure of how well a parameter has been determined is given by the probability distributions. However, if the reliability of the solution for each parameter should be quantified in a single number the best measure is the standard deviation measured by the length of the search interval for each parameter $\sigma_i/(F\ \max_i - F\ \min_i)$ (see Table 3). This estimate describes how the solutions are clustered over the search interval, and the table has been ordered by increasing uncertainty for the parameters. A change in the span of the search interval for a parameter will clearly change the parameter's relative importance.

Table 3. The standard deviation for the general mismatch case. The standard deviation for each parameter is measured in terms of the length of the search interval for the parameter.

Parameter	40 dB	10 dB	−5 dB
Source depth	0.001	0.005	0.000
Source range	0.003	0.024	0.039
Water speed decrease	0.004	0.041	0.083
Upper sediment speed	0.025	0.047	0.189
Water depth	0.031	0.121	0.276
Density	0.023	0.084	0.279
Attenuation	0.035	0.044	0.192
Lower sediment speed	0.065	0.070	0.303
Top water speed	0.072	0.298	0.191

4.2. *Sloping bottom*

The sloping bottom case was solved assuming a range-independent environment. There are two reasons for this. First we can still use a standard mode code and secondly we can investigate the error introduced by using a wrong discretization. Thus the same discretization and computational setup was used as for the general mismatch. Solving this problem, without taking the slope of the bottom into account, represents a case of incomplete discretization of the environment, and the problem can be solved using a simpler and less CPU intensive forward modeling method. This incorrect discretization will give an increase in unwanted signal. The best fit parameters are given in Table 4 and for the 10 dB and the −5 dB SNR the *a posteriori* probability distributions are presented in Fig. 8. For the 10 dB and the −5 dB SNR the error in the source depth is 2 m and in the source range is 200 m. For the

Table 4. The best fit parameters for the sloping bottom case.

Parameter		Estimated values			True values		
		40 dB	10 dB	−5 dB	40 dB	10 dB	−5 dB
Source depth	(m)	68	70	56	70	72	58
Source range	(km)	5.5	5.8	7.9	5.7	6.0	8.1
Top water speed	(m/s)	1498.0	1498.0	1498.3		1497.9	
Water speed decrease	(m/s)	20.5	20.4	20.4		19.6	
Water depth	(m)	100.3	100.5	101.4		101.2–104.6	
Upper sediment speed	(m/s)	1606	1606	1620		1604	
Lower sediment speed	(m/s)	1726	1842	1658		1798	
Attenuation	(dB/λ)	0.10	0.10	0.11		0.11	
Density	(g/cm^3)	1.71	1.63	1.63		1.65	
Bartlett power	(dB)	13.0	13.0	12.8			

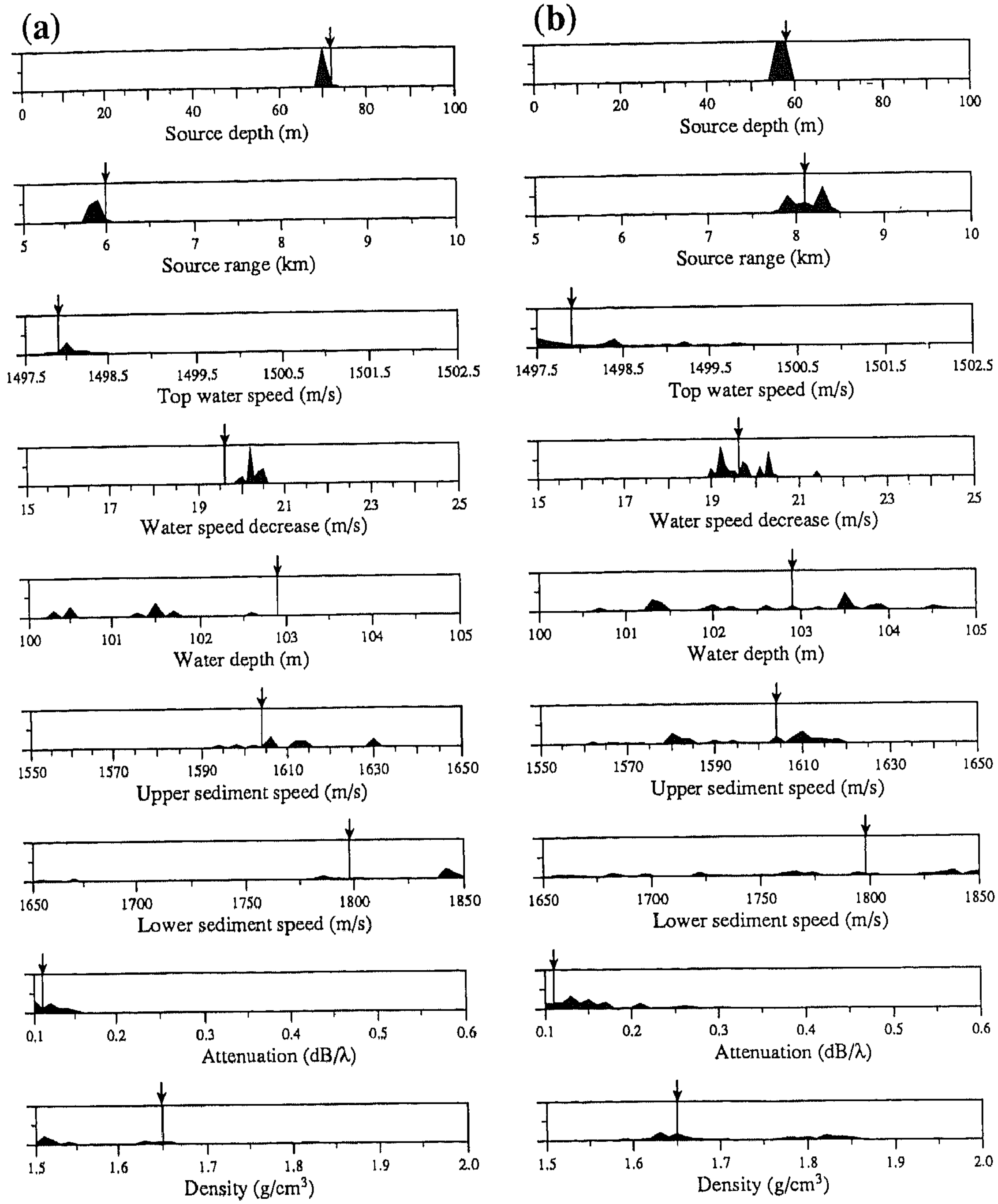

Fig. 8. Probability distribution for the sloping bottom case based on the discretization of the water speed by shape functions. (a) 10 dB SNR, (b) −5 dB SNR. The arrows indicate the correct values.

water depth, the true depth at the receiving array is 101.2 m and at 10 km it is 104.6 m. As the source is located at 6.0 km (10 dB) or 8.1 km (−5 dB) the inverted average water depth should be closer to the water depth at the receiving array, and this is the case for the 10 dB case. For the −5 dB case the determined average depth is more spread out. This is probably due to both a more distant source and a lower SNR. Even though the probability distributions indicate that the sediment values are not very reliable it is seen from Table 4 that the best fit parameters satisfactorily correspond to the true ones. It is also seen that the accuracy of the estimated parameters is about the same for all the three SNR's.

5. Summary and Conclusions

A global inversion has been carried out using the approach described by Gerstoft.[2] Genetic algorithms have been used for the optimization and the results are presented using *a posteriori* probability distributions whereby the accuracy and importance of the parameters can be assessed.

It was demonstrated that it is very important how the environment is described; specifically the water sound speed is better modeled by a constant value plus a slope as opposed to the upper and lower speeds in the water. For high SNR we are able to retrieve both the source and the environmental parameters. As the SNR decreases the less important parameters become undetermined.

It is clear that it is feasible to invert synthetic data like these, even for low SNR when the parametrization of the environment is given. For real data we have to make several choices since a proper description of the environment requires thousands of parameters, and we are still only able to use a few of these in an inversion. It is important to know which parameters are the important ones. Thus there is a large step from synthetic data inversion to a real data inversion. The present work is focused on how to discretize the environment and to determine the effect of a wrong discretization.

Acknowledgments

The author wishes to thank Don Gingras and Finn Jensen for their invaluable comments which improved the quality of this paper.

References

1. M. Porter and A. Tolstoy, "The matched field processing benchmark problems," *J. Comput. Acous.* **2** (1994) 161–185.
2. P. Gerstoft, "Inversion of seismo-acoustic data using genetic algorithms and *a posteriori* probability distributions," *J. Acous. Soc. Am.* **95** (1994) 770–782.
3. M. B. Porter, R. L. Dicus, and R. G. Fizell, "Simulations of matched-field processing in a deep-water Pacific environment," *J. Acous. Soc. Am.* **86** (1989) 1940–1949.
4. D. F. Gingras, "Methods for predicting the sensitivity of matched-field processing to mismatch," *J. Acous. Soc. Am.* **86** (1989) 1940–1949.
5. A. Tolstoy, "Sensitivity of matched field processing to sound speed profile mismatch for vertical arrays in a deep water Pacific environment," *J. Acous. Soc. Am.* **85** (1989) 2394–2404.

6. M. D. Collins and W. A. Kuperman, "Focalization: Environmental focusing and source localization," *J. Acous. Soc. Am.* **90** (1991) 1410–1422.
7. A. M. Richardson and L. W. Nolte, "*A posteriori* probability source localization in an uncertain sound speed deep ocean environment," *J. Acous. Soc. Am.* **89** (1991) 2280–2284.
8. D. F. Gingras and N. L. Gerr, "Minimax robust matched-field processing," *J. Acous. Soc. Am.* **93** (1993) 2798–2808.
9. A. B. Baggeroer, W. A. Kupermann, and H. Schmidt, "Matched field processing: Source localization in correlated noise as an optimum parameter estimation problem," *J. Acous. Soc. Am.* **93** (1993) 2798–2808.
10. L. Davis, ed., *Handbook of Genetic Algorithms* (Van Nostrand Reinhold, New York, 1991) (ISBN 0-442-00173-8).
11. F. B. Jensen and M. C. Ferla, "SNAP: The SACLANTCEN normal-mode acoustic propagation model," SM-121, SACLANT Undersea Research Centre, La Spezia, Italy, 1979.
12. J. A. Scales, M. L. Smith, and T. L. Fisher, "Global optimization methods for highly nonlinear inverse problems," *J. Comput. Phys.* **103** (1992) 258–268.
13. M. Sambrigde and G. Drijkoningen, "Genetic algorithms in seismic waveform inversion," *Geophys. J. Int.* **109**, 323–343 (1992).
14. P. L. Stoffa and M. K. Sen, "Multiparameter optimization using genetic algorithms: Inversion of plane wave seismograms," *Geophys.* **56** (1991) 1794–1810.
15. M. K. Sen and P. L. Stoffa, "Rapid sampling of model space using genetic algorithms: Examples from seismic waveform inversion," *Geophys. J. Int.* **108** (1992) 281–292.
16. L. R. LeBlanc and F. H. Middleton "An underwater acoustic sound velocity data model," *J. Acous. Soc. Am.* **67** (1980) 2055–2062.
17. S. D. Rajan, J. F. Lynch, and G. V. Frisk, "Perturbative inversion methods for obtaining bottom geoacoustic parameters in shallow water," *J. Acous. Soc. Am.* **82** (1987) 998–1017.
18. A. B. Baggeroer and H. Schmidt, "Parameter estimation bounds on estimating geophysical parameters using matched-field tomography," *J. Acous. Soc. Am.* **93** (1993) 2400.